Correlation of the lattice distortion and polaron conduction with tile physical properties of $La_{0.7}Ca_{0.3}MnO_3$ and $La_{0.5}Ca_{0.5}CoO_3$ epitaxial films

N.-C. Yeh[1], R. P. Vasquez[2], C.-C. Fu[1], J. T. Y. Wei, H. Huynh[1], S. M. Maurer[1], D. A. Beam[1], and G. Beach[1]

[1]Department of Physics, California institute of 'J'ethnology, Pasadena, CA 91125

[2]Center for Space Microelectronics '~'ethnology, Jet Propulsion Laboratory, California Institute of Technology, Pasadena, CA 91109

The effects of lattice distortion on the physical properties of $La_{0.7}Ca_{0.3}MnO_3$ epitaxial films are investigated. Our results suggest that larger substrate-induced lattice distortion gives rise to larger zero-field resistivity and larger negative magnetoresistance. Similar effects are also observed in samples of different thicknesses and on the same substrate material, with larger resistivity anti magnetoresistance associated with thinner samples. In addition to x-ray diffraction spectroscopy, the degrees of lattice distortion in different samples are further verified by the surface topography taken with a low-temperature scanning tunneling microscope. Quantitative analyses of the transport properties suggest that the high-temperature (T -, T_C) colossal magnetoresistance (CMR) in the manganites is consistent with the conduction of lattice polarons induced by the Jahn-Teller coupling, and that the low-temperature ($T << T_C$) magnetoresistance may be attributed to the magnetic domain wall scattering. In contrast, the absence of the Jahn-Teller coupling and the large conductivity in $La_{0.5}Ca_{0.5}CoO_3$ epitaxial films yield much smaller negative magnetoresistance which may be attributed to disorder-spin scattering.

PACS: 75.70.-i, 73.50.-h

Recent experimental studies of the colossal magnetoresistive manganites $Ln_{1-x}A_xMnO_{3-\delta}$ (Ln: trivalent rare earth ions, A: divalent alkaline earth ions) have led to new information which suggests the relevance of lattice effects on the! conductivity and magnetism of these manganites[1-5]. Some representative experimental observation includes a strong correlation between the thickness of epitaxial films and the corresponding magnetoresistance[1]; decreasing Curie temperatures (T_C) and increasing CMR effects with the increasing lattice distortion via the substitution of La ions by smaller ions of Pr and Y[2]; a significant reduction of the magnetoresistance in single crystals under a hydrostatic pressure[3]; as well as a large magnetovolume effect[4] and a giant oxygen isotope effect[5] in $La_{1-x}Ca_xMnO_3$. On the physical origin for the colossal magnetoresistance (CMR), the importance of lattice polaron conduction incurred by the Jahll-Teller coupling in the manganites has been proposed[6].

In this work, we explore the correlation of the lattice distortion and Jahn-Teller coupling with the magnetoresistance of $La_{0.7}Ca_{0.3}MnO_3$ (LCMO) and $La_{0.5}Ca_{0.5}CoO_3$ (LCCO) epitaxial films. The lattice distortion is varied by either growing films of the same thickness on substrates with various lattice constants, or by varying the thickness and the growth rate of the film on the same type of substrate. The correlation between the Jahn-Teller coupling and the occurrence of CMR is investigated by comparing the physical properties of LCMO and LCCO epitaxial films grown under the same conditions. This comparison is based on the fact that cobaltites with doping levels between 0.4 and 0.6 are known to be ferromagnetic metals which are isostructure to the manganites and are without the Jahn-Teller coupling[7,8]. The substrates selected include single crystalline $LaAlO_3$ (LAO), $SrTiO_3$ (STO), and $YAlO_3$ (YAO). These substrates are chosen to provide a range of lattice constants which allows studies of the effects of tensile and compressive stress of the films.

The LCMO and LCCO epitaxial films are grown by pulsed laser deposition using stoichiometric targets. For studying the substrate-induced lattice distortion, 200 nm thick films on different substrates are grown in 100 mTorr of oxygen with the substrate temperature at 700° C, and subsequently annealed at 900° C of 1 atm oxygen for two hours. The Curie temperature T_C for all LCMO is 260 ± 10 K, and that for the LCCO is $T_C = 150 \pm 5$ K. The lattice constants a, b and c ($c \perp$ sample surface) as well as the epitaxy of the films are deter-

mined using high resolution x-ray diffraction spectroscopy and x-ray rocking curves, and the results have been given elsewhere[9]. Another batch of LCMO films are grown on LAO with a thickness of 100 nm, and under the same conditions described above except for two different growth rates controlled by the laser fluent.es. Among both the LCMO and LCCO films of the same thickness, wc find the largest lattice distortion in LCMO/YAO and LCCO/YAO from the x-ray data[9]. For LCMO/LAO samples with different thicknesses and under different growth rates, the thinner sample of 100 nm is found to exhibit larger lattice distortion. The chemical properties of these samples arc further characterized with x-ray photoelectron spectroscopy (X I'S)[1 O]. The room-temperature valence band spectroscopy shows no density of states at the Fermi level for the manganites and a high density of states at the Fermi level for the cobaltites[1 O], consistent with the semiconducting nature of the former and metallic nature of the latter.

The effects of lattice distortion on the magnetoresistance ΔR_H of the LCMO films of the same thickness (200 nm) arc illustrated in F'ig.1 for $H = 6$ Tesla, with the magnetoresistance in a magnetic field H defined as $\Delta R_H \equiv [\rho(H) - \rho(0)]/\rho(H)$. The correlation of surface topography with the magnetoresistive behavior of the sample is investigated via STM imaging. In Fig.2 the STM surface topography of LCMO/LAO and LCMO/STO films shows images with atomically smooth surfaces and highly oriented rectangular terrace steps which are correlated with the substrate and the crystalline axes. According to our x-ray data and the transport measurements[9], the LCMO/LAO and LCMO/STO samples exhibit overall comparable lattice distortion and magnetoresistance, although the lattice distortion and the maximum magnetoresistance for LCMO/STO are slig htly larger. These results are consistent with the STM surface topography in Fig. ? which shows comparable surface roughness[11] for the two samples, with a slightly higher step density in the LCMO/STO film. Similar correlation of the surface topography with the electrical transport properties is also observed in the case of LCMO/LAO films of different thicknesses and growth rates. .4s shown in Figs.3 and 4, the magnetoresistance of three I, CMO/LAO films appear to be correlated with the mcIrphology of the surface, with the magnetoresistance of the thinner samples (1 00 nm) significantly larger than those of the thicker LCMO/LAO sample (?00 nm), and the surface topography

of the thinner sample appears noticeably more irregular. It is also interesting to note that the thin sample (100 nm) under a slower growth rate (1 .6J/cm^2 laser fluence) shows both step-flow and island growth modes, whereas the faster growth rate (2 J/cm^2 laser fluence) yields a predominantly island growth mode.

Assuming polaron conduction as the dominant conduction mechanism for LCMO at high temperatures, the resistivity data for all LCMO films are analyzed according to the expression:

$$\rho(T) \approx \alpha T \exp\left[\frac{E_b(T)}{k_B T}\right], \quad (1)$$

where E_b is the polaron binding energy, α a constant, and the temperature and magnetic field dependence of E_b satisfies the conditions imposed by the polaron model. That is, $E_b \to 0$ in the limit of complete magnetic order when the increasing hopping rate of the itinerant electrons exceeds the optical phonon frequency, and $E_b \to E_{b0} \sim$ constant in the absence of long-range magnetic order. For all LCMO films, the fitting to the high-temperature resistivity data yields $E_{b0} \approx 0.35$ eV[9]. This energy compares favorably to the Jahn-Teller coupling energy[6], suggesting that the high- temperature conduction mechanism is dominated by the lattice polaron conduction.

On the other hand, the low temperature transport properties appear to be strongly correlated with the degree of lattice distortion. That is, samples of larger lattice distortion exhibit larger resistivity and magnetoresistance, suggesting increasing electron scattering due to a larger number of magnetic domains and grain boundaries induced by larger lattice distortion. The incompletely aligned moments of the magnetic domains due to either inhomogeneity or pinning by local defects below T_C give rise to larger scattering of conduction electrons. Therefore an applied magnetic field has more significant effects on aligning the magnetic domains, thereby more effectively reducing the resistivity in samples with larger lattice distortion.

To investigate the relevance of lattice polarons to the occurrence of CMR effects, the resistivity and magnetization of LCCO films on LAO and YAO substrates were studied. Despite comparable lattice relaxation and lattice strain in the manganites and in LCCO/YAO[9], the magnitude and temperature dependence of the resistivity in the LCMO and LCCO systems exhibit sharp contrasts, as illustrated in Figs.1 and 5. Also shown in Fig.5, for the LCCO/YAO sample, a faster decrease in the zero-field resistivity as well as a maximum in

the magnitude of negative magnetoresistance both occur at approximately the Curie temperature ($T_C \approx$ 180 K), suggesting that magnetic. ordering below T_C reduces the resistivity[9]. Our recent studies of the anomalous Hall effect[12] on the LCCO sample also confirm that the magnetoresistance in LCCO is of the origin of disorder-spin scattering rather than polaron conduction.

In summary, we have studied the effects of lattice distortion on the physical properties of $La_{0.7}Ca_{0.3}MnO_3$ epitaxial films by varying the thickness of films on the same substrate, and by depositing the same thickness of films on various substrates with a range of lattice constants, Our studies reveal that larger substrate-induced lattice distortion gives rise to larger zero-field resistivity and larger negative magnetoresistance. The lattice distortion determined from the x-ray diffraction studies is further confirmed by the STM images of the surface topography. Our results suggest that the high-temperature ($T \rightarrow T_C$) CMR in the manganites is consistent with the conduction of lattice polarons induced by the Jahn-Teller coupling, and that the low-temperature ($T << T_C$) negative magnetoresistance can be attributed to the magnetic domain wall scattering. In contrast, the absence of the Jahn-Teller coupling and the large conductivity in $La_{0.5}Ca_{0.5}CoO_3$ epitaxial films may account for the much smaller negative magnetoresistance.

The research at Caltech is supported by the Packard Foundation and the National Aeronautics ant! Space Administration, Office of Space Access and Technology (NASA/OSAT). Part of the research was performed by the Center for Space Microelectronics Technology, Jet Propulsion Laboratory, Caltech, and was sponsored by NASA/OSAT. We thank Nikko Hitech International Inc. for supplying the $YAlO_3$ substrates used in this work.

REFERENCES

[1] S. Jin, T. H. Tiefel, M. McCormack, R. A. Fastnacht, R. Ramesh, and I,. H. Chen, Science 264, 413 (1994); Appl. Phys. Lett. 66, 382 (1995); Appl. Phys. Lett. 67, 557 (1995).

[2] H. Y. Hwang, S.-W. Cheong, P. G. Radaelli, M. Marezio, and B. Batlogg, Phys. Rev. Lett. 75, 914 (1995).

[3] K. Khazeni, Y. X. Jia, I,. Lu, V. H. Crespi, M. I,. Cohen, and A. Zettle, Phys. Rev. Lett. 76, 295 (1996).

[4] M. R. Ibarra, P. A. Algarabel, C. Marquina, J. Blasco, and J. Garcia, Phys. Rev. Lett. 75, 3541 (1995).

[5] G.-M. Zhao, K. Conder, H. Keller, and K. A. Müller, Nature 381, 676 (1996).

[6] A. J. Millis, P.B. Littlewood, and B. I. Shraiman, Phys. Rev. Lett. 74, 5144 (1995); A. J. Minis, B. I. Shraiman, and R. Mueller, Phys. Rev. Lett. 77, 175 (1996).

[7] H. Ohbayashi, T. Kudo and T. Gejo, Jpn. J. Appl. Phys. 13, 1 (1974).

[s] R. Mahendiran et al., J. Phys.: Condens. Matter 7, L561 (1995); S. Yamaguchi et al., J. Phys. Sot. Jpn. 64, 1885 (1995).

[9] N.-C. Yeh, R. P. Vasquez, D. A. Beam, C.-C. Fu, H. Huynh, and G. Beach, submitted to Phys. Rev. R.

[10] R. P. Vasquez, Phys. Rev. B, (in press).

[11] For the definition of the surface roughness, see, for example, M. Ohring, "*The Material Science of Thin Films*", Academic Press Inc., San Diego, CA, (1992).

[12] A. V. Samoilov, N.-C. Yeh and R. P. Vasquez, submitted to Science.

Fig.1 The effect of lattice distortion on the magnetoresistance ΔR_H as a function of the temperature is shown for $La_{0.7}Ca_{0.3}MnO_3$ epitaxial films on different substrates of $LaAlO_3$, $YAlO_3$, and $SrTiO_3$. Here the applied field is $H = 6.0$ Tesla.

Fig.2 STM images of 200 nm thick LCMO epitaxial films 011 (a) LAO and (b) STO substrates, showing highly oriented rectangular terrace structures formed by step-flow growth mode. The images are 100nm × 100nm in size and 0.12 nm in grey scale, indicating rms surface roughness of 0.4 nm for (a) and 0.3 IiII-l for (b). The terrace steps are typically 0.8 or 0.4 nm in height, consistent with either the unit cell or half-relit-cell lattice parameter.

Fig.3 Comparison of the thickness and growth rate dependence of tile magnetoresistance $\Delta R_H(T)$ with $H = 6.0$ Tesla in LCMO/LAO films. The inset shows the corresponding zero-field resistivity $\rho(T)$ of the same samples.

Fig.4 STM images of 10011111 thick LCMO epitaxial films grown on LAO substrates at (a) 2 J/cm^2 and (b) 1.6 J/cm^2 laser fluence. The images are 150nm x 150nm in size and the grey scales are 0.35 nm for (a) ant] 0.25nm for (b), with rms surface roughness of 0.5 nm and 0.3 nm, respectively. The higher growth-rate sample (a) shows rounded "rice-paclcly" terraces indicating island growth mode. The lower growth-rate sample (b) shows jagged "fish-scale" terraces suggesting a more step-flo~v growth mode. The terrace steps are typically 0.S nm or 0.4 nm in height, consistent with either the unit-cell or half-unit-cell lattice parameter. The more distorted surface morphology of the 100 nm fil ms as compared with the 200 nm films [Fig.2] is consistent with the higher lattice distortions in the former.

Fig.5 The zero-field resistivity ρ and the magnetoresistance ΔR_H of a LCCO/LAO film, showing strong correlation of the magnetoresistance with spin fluctuations near T_C.

Figure 1

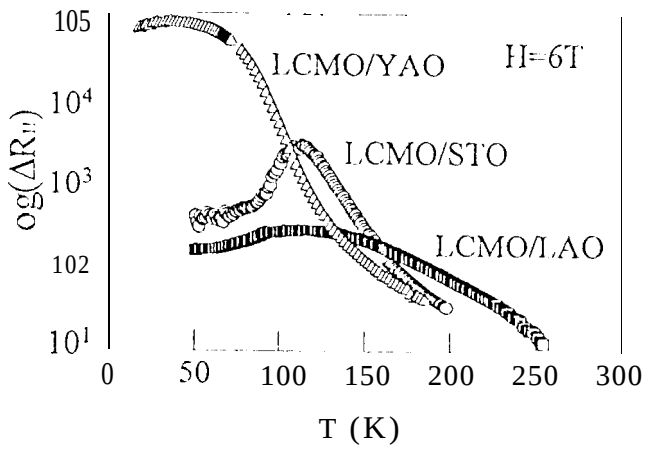
105
10^4
10^3
102
10^1
og($\Delta R_{//}$)
LCMO/YAO
H=6T
LCMO/STO
LCMO/LAO
0
50
100
150
200
250
300
T (K)

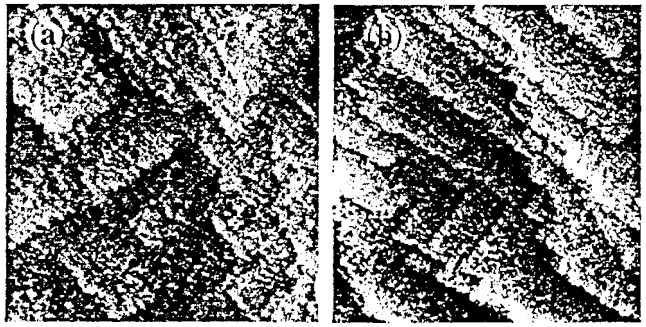

Fig.2 STM images of 200 nm thick LCMO epitaxial films grown on (a) LAO and (b) STO substrates, showing highly oriented rectangular terrace structures formed by step-flow growth mode. The images are 100nm x100nm in size and 0.12 nm in grey scale, indicating rms surface roughness of 0.4 nm for (a) and 0.3 nm for (b). The terrace steps are typically 0.8 or 0.4 nm in height, consistent with either the unit-cell or half-unit-cell lattice parameter.

Figure 3

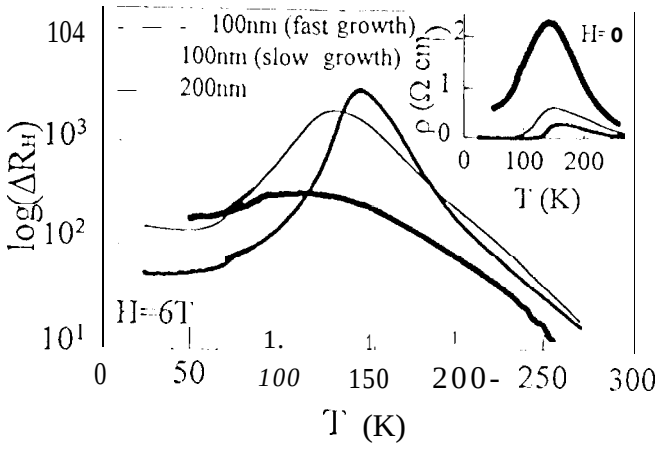
104
10^3
10^2
10^1
$\log(\Delta R_H)$
100nm (fast growth)
100nm (slow growth)
200nm
H=6T
H=0
ρ (Ω cm)
2
1
0
0 100 200
T (K)
0 50 100 150 200 250 300
T (K)

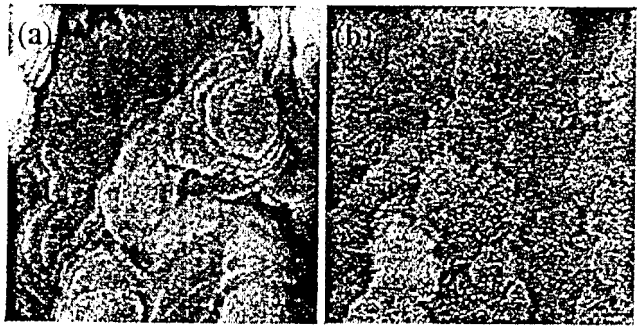

Fig.4 STM images of 100 nm thick LCMO epitaxial films grown on LAO substrates at (a) 2 J/cm^2 and (b) 1.6 J/cm^2 laser fluence. The images are 150nm x150nm in size and the grey scales are 0.35nm for (a) and 0.25nm for (b),with rms surface roughness of 0.5nm and 0.3 nm respectively. The higher growth-rate sample (a) shows rounded "rice-paddy" terraces indicating island growth mode. The lower growth-rate sample (b) shows jagged "fish-scale" terraces suggesting a more step-flow growth mode. The terrace steps are typically 0.8 or 0.4 nm in height, consistent with either the unit-cell or half-unit-cell lattice parameter. The more disordered surface morphology of the 100nm films as compared with the 200 nm films [Fig.2] is consistent with the higher lattice distortions in the former.

Figure 5

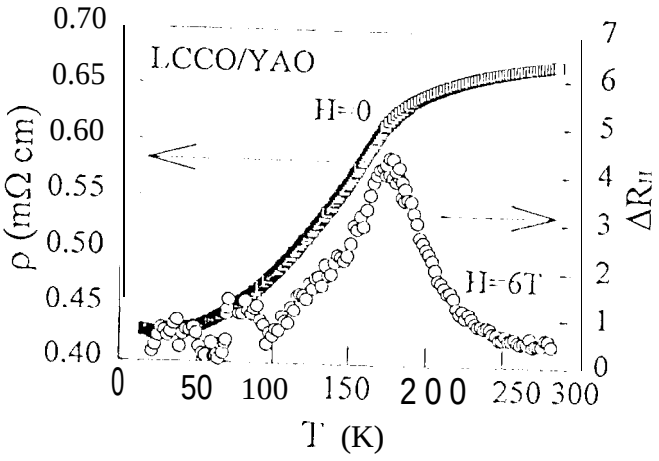
LCCO/YAO
H=0
H=6T
ρ (mΩ cm)
ΔR_H
T (K)
0.70
0.65
0.60
0.55
0.50
0.45
0.40
7
6
5
4
3
2
1
0
0
50
100
150
200
250
300